Nevis - 7
R - 101
CU - 80

Nevis Cyclotron Laboratories
Columbia University
Department of Physics
New York, New York

A DIFFUSION CLOUD CHAMBER STUDY OF VERY SLOW MESONS: II. BETA DECAY OF THE MUON

C.P. Sargent, M. Rinehart,
L.M. Lederman and K.C. Rogers

CU-80-55-ONR-110-1-Physics

March, 1955

Joint ONR-AEC Program
Office of Naval Research Contract
Contract N6-ori-110-Task No.1

DISCLAIMER

A Diffusion Cloud Chamber Study of Very Slow Mesons;*
II. Beta Decay of the Muon

C. P. Sargent,** M. Rinehart, L. M. Lederman and K. C. Rogers

Department of Physics, Columbia University
New York, New York

March, 1955

---

* This research was supported in part by the joint program of the Office of Naval Research and the Atomic Energy Commission.

** Now at Laboratory for Nuclear Science, Massachusetts Institute of Technology, Cambridge, Massachusetts.

ABSTRACT

The spectrum of electrons arising from the decay of the negative mu meson has been determined. The muons are arrested in the gas of a high pressure hydrogen filled diffusion cloud chamber. The momenta of the decay electrons are determined from their curvature in a magnetic field of 7750 gauss. The spectrum of 415 electrons has been analyzed according to the theory of Michel. The shape parameter, ρ, is found to be $0.64 \pm .10$. The significance of this result in terms of the beta interaction is discussed.

A. INTRODUCTION

The determination of the spectrum of electrons which are produced by the decay of the muon is one of the most honored problems in particle physics.[1-10] Some of the difficulties in arriving at

---

1 R. Thompson, Phys. Rev. 74, 490 (1948)

2 J. Steinberger, Phys. Rev. 75, 1136 (1948)

3 Leighton, Anderson and Seriff, Phys. Rev. 75, 1432 (1949)

4 A. Lagarrique and C. Reyrou, Compt. Rend. 233, 478 (1951)

5 Davies, Lock and Muirhead, Phil. Mag. 40, 1250 (1949)

6 Sagane, Gardner and Hubbard, Phys. Rev. 82, 557 (1951)

7 H. Bramson and W. Havens, Phys. Rev. 88, 304 (1952)

8 R. Levisetti and G. Tomasini, N. Cim., 8, 12 (1951)

9 J. Vilain and R. Williams, Phys. Rev. 94, 1011 (1954)

10 Sagane, Dudziak and Vedder, Phys. Rev. 95, 863 (1954)

---

definite conclusions from the mass of data are discussed by Williams.[9] One of the principal difficulties is the generally poor resolution that has been used. The earlier data were not accompanied by detailed discussions of the resolution of the respective techniques. The lack of resolution was principally due to radiation losses of the decay electrons in the material used to arrest the muons.

The present experiment employs the gas of a hydrogen filled diffusion cloud chamber working at a pressure of 19 atmospheres, to stop negative muons and to observe the momentum of the decay electrons. The experimental arrangement has already been reported.[11] In addition to the negligible radiation and ionization los-

---

[11] Sargent, Cornelius, Rinehart, Lederman and Rogers. In Press. Referred to as I.

---

ses, the lack of dead mass allows an examination of the entire spectrum. This virtue eliminates the necessity of arbitrarily normalizing the data.

B. EXPERIMENTAL CONSIDERATIONS

Negative mesons from the 60 Mev pion beam of the Nevis Cyclotron are moderated and allowed to enter the diffusion chamber, where a small fraction of pions and muons spiral to rest in the gas. (See Fig. 1) Muon endings are scanned for associated decay-electrons. Momenta of the electrons are determined from curvature and angle measurements and from the value of the magnet field ($\bar{H}$ = 7750 gauss) at the time of the event.

Because of the finite depth of the sensitive layer the visible path length of roughly half of the decay electrons is so short that their inclusion in the data would seriously impair momentum resolution. The mesons decay from Bohr orbits, hence any criterion which requires that the electrons be emitted within some specified solid angle with respect to any direction in space will not bias the momentum spectrum. A dip angle versus height relation constituted the criterion for acceptance of decay events for measurement. For example, an electron starting at the top of the sensitive layer was required to be moving down with a dip angle of less than 48°: $0 < \tan\alpha < 1.1$.

Few of the accepted tracks were shorter than 8 cm. The average electron track was 12 cm in length. In the 15-50 Mev/c momentum range, the 8 cm track in 7750 gauss was measurable to about 5 percent. The error varies inversely as the square of the projected track length.

A monochromatic electron beam of appropriate momentum for investigating resolution was not available. However, one may assign a reasonably good estimate of the momentum uncertainty to each momentum measurement. The distribution of such uncertainties determines a momentum resolution function. Appendix I describes the momentum measurement procedure, the uncertainties involved in the measurements and the determination of the resolution functions.

C. EXPERIMENTAL RESULTS

Fig. 2 represents the distribution of 415 decay electrons. The number of events per unit momentum interval is plotted against electron momentum. The horizontal bar attached to each point indicates the momentum interval Δp, used to determine the point. The intervals are chosen sufficiently small that no significant error is made in placing the point at the center of the interval, if one assumes the spectrum to be a smoothly varying function of momentum. The vertical bar attached to each point is a measure of the statistical reliability of the point. It extends $\sqrt{(\Delta N + 1)}/\Delta p$ from the point, where ΔN is the number of events in the electron momentum interval Δp.

The curves above the momentum scale in Fig. 2 are resolution functions at 20 and 50 Mev/c. The resolution function at momentum p represents the distribution of momenta which would be observed from a monochromatic source of electrons with momentum p. These are determined by the method of Appendix I. The resolution function at momentum p turns out to have a width at half maximum given by $R = (.066 \pm .020)\ p$. Fig. 3 illustrates the results of improving the resolution by a more stringent set of criteria. These further limit the solid angle for acceptable tracks. The resulting tracks are less steeply inclined to the horizontal and are longer. This division of the data is useful in studying the propagation of resolution errors.

D. ANALYSIS OF DECAY SPECTRUM

The reaction being observed has been interpreted as following the scheme:

$$\mu^- \rightarrow e^- + \nu + \nu \qquad (1)$$

The theory of this reaction has been developed by Tiomno, Wheeler and Rau[12] and by Michel.[13] The reaction (1) is a weak interaction

---

12 Tiomno, Wheeler and Rau, Revs. Mod. Phys. 21, 144 (1949)

13 L. Michel, Nature 163, 959 (1949); Thesis, Paris (1950), Proc. Phys. Soc. (London) A63, 514 (1950)

---

of four spin 1/2 particles and is treated in the same way as the nuclear beta decay interaction. Michel's results are given to excellent approximation by the spectral distribution:

$$P(x) = 4x^2\ [3(1-x) + 2/3\ \rho(4x-3)] \qquad (2)$$

where P(x)dx is the probability per unit time for the decay at rest of a muon producing an electron with momentum between p and p + dp, $x = p/W$, and W is one half the muon rest mass. The parameter ρ is a function of the interaction coupling constants and, in Michel's theory, may have values between 0 and 1. Experimental examination of the electron spectrum can then determine but the single parameter ρ.

The right side of Eq. 2 must be modified before it is compared with experiment. The negative mesons are not at rest when they decay. From a study of stars made by stopped pions and muons,[14] we

---

[14] C. P. Sargent, Thesis, Columbia University (1953)

---

have established that 35 ± 15 percent of the muons decay from the K shell of mesic oxygen, nitrogen or carbon which constitute a 0.4 percent impurity in the gas. The remainder decay from the K shell of mesic hydrogen. The large fraction decaying from the impurity arises from the long lifetime of mesic hydrogen and the large cross section for collisions in which the muon is transferred to the impurity. Porter and Primakoff[15] have calculated the expected

---

[15] Porter and Primakoff, Phys Rev , 83, 849 (1951)

---

spectrum shape for a meson decaying from a 1s orbit about a nucleus of charge Z.

Their result, $P'(x)$ for $Z < 10$, is essentially represented by smearing $P(x)$ with a bell-shaped resolution function $R_1(\sigma,x)$ which has a width at half maximum $\sigma = \alpha(Z/2)\,x$, $\alpha = 1/137$. Thus

$$P'(x) = \int_0^\infty R_1(\sigma,\, x-y)\, P(y)\, dy \qquad (3)$$

Actually, the equations of reference 15 were used to compute $P'(x)$.

The second modification is the experimental resolution function $R_2(x)$ (Appendix I). Thus

$$P''(x) = \int_0^\infty R_2(x-y)\, P'(y)dy \qquad (4)$$

This is much more important than R_1. $P''(x)$ is plotted in Fig. 4 for ρ = 0, 1/4, 1/2, 3/4 and 1 along with the experimental points.

It is necessary to see whether the data is adequately represented by a curve with some value of ρ and, if such is the case, to define a measure of the reliability of the empirically determined ρ. Assuming the data to represent an unbiased sampling of the μ-electron decay spectrum, there remain five sources of error to consider in comparing theory with experiment.

i) The uncertainty in the vertical position of the points in Fig. 2 which result from the finite number of events observed in a given momentum interval.

ii) The uncertainty in the horizontal position of the points which results from conversion of radius of curvature measured in reprojection to electron momentum. The conversion goes via a 'momentum scale factor' denoted by H. The uncertainty ΔH in H arises from a lack of precise knowledge of the magnetic field and from imperfect reprojection. Since the field is known to 1.0 percent and the fiduciary mark spacing is reproduced in reprojection to 0.5 percent, $\Delta H/H$ = .011.

iii) The uncertainty, both vertical and horizontal in the position of the points which result from a lack of knowledge of

$W = \mu/2$. We take $\mu = 207.0 \pm 1.0$ and $\Delta W/W = 0.005$. The analysis assumes that two zero rest mass neutrinos are emitted in the decay.

iv) The uncertainty in the position of the curves which result from lack of precise knowledge of the half-width R and the shape S of the momentum resolution function. We find $\Delta R/R \approx 0.35$ for the data of Fig. 2. In order to minimize this effect, we have also computed ρ from the better resolution data of Fig. 3. In this way, statistics are traded for resolution in order to uncover any possible large systematic effects which could arise from finite resolution.

The simplest method of obtaining the shape parameter, ρ, from the data is by the method of moments.[16] This method, although

---

[16] The i^{th} moment is $\bar{X}_i = \int_0^\infty x^i \, P(x) \, dx$

---

statistically not efficient, gives the propagation of various errors quite simply.

Table I summarizes the results of various estimates based on moments. Only the major uncertainties are displayed here.

In Table I $\Delta\rho_H$ is the contribution to the uncertainty $\Delta\rho$ due to the horizontal scale error ΔH. $\Delta\rho_S$ is the statistical standard deviation. The split moment is designed to uncover a systematic error in the scale H.

To use the data more efficiently, a least squares analysis has been performed in order to determine ρ and to test the theoretical shape with the best value of ρ determined. To do this, the sum

$$M = \sum_i \frac{[N_{obs}(x_i) - N_{Michel}(\rho, x_i)]^2}{N_{obs}(x_i)}$$

0390 009

has been evaluated for each of the five curves of Fig. 4. The results are plotted for the poor resolution data in Fig. 5. The curve is fitted by a parabola and the minimum thus determined. The result is:

$$\rho = 0.64 \pm .09 \quad \text{(Standard deviation)}$$

The various confidence levels are indicated on the graph.

The minimum value of $\chi^2[=M(\rho = .64)]$ is 18 for 18 intervals and one parameter. This agrees well with the statistically expected average chi square which is 16.

Finally it is necessary to investigate the sensitivity of ρ to the uncertainties ΔH, ΔW, ΔR, ΔS, and ΔF. This is accomplished by varying the indicated parameters by given amounts, which changes the position of either the points or the curves of Fig. 4, and then recalculating ρ.

The results are:

$$\Delta\rho_H = |+ 3.5\ \Delta H/H| = 3.5 \times .011 = .039$$

$$\Delta\rho_W = |- 2.8\ \Delta W/W| = 2.8 \times .005 = .014$$

$$\Delta\rho_R = 4.4 \times 10^{-2}\ \Delta R/R = .044 \times .35 = .015$$

If S is Gaussian ρ is changed by less than 0.005; if F = 1 (all mesons decay from oxygen) ρ is changed by less than 0.01. The sensitivity of ρ to improvement of the resolution is indicated in Table I and in a comparison of Fig. 2 and 3. The results show that the resolution curve of Fig. I contains an undetected 'tail' which probably accounts for the events between 65 and 80 Mev.[17] The origin of this

---

17. The possibility of competing events e.g. $\mu^- + O^{16} \rightarrow (O^{16})^* + e^-$

contributing to this tail has been ruled out by a recent experiment of Steinberger, Wolfe and Lokanathan, private communication.

---

tail probably arises from track distortions, not observed in zero field studies which are carried out on flat tracks. The results of Table 1 indicate that no large error is introduced by the unknown and possibly asymmetric tail in the resolution function.

Combining all uncertainties, we find

$$\rho = 0.64 \pm .10 \quad \text{(Standard deviation)}$$

D. DISCUSSION

There has been disagreement between values of ρ obtained by different experiments. Vilain and Williams have examined the decay spectrum of positive muons with an expansion cloud chamber and have found $\rho = 0.50 \pm 0.12$, a value which agrees both with the present work on negative muon decay and with the earlier photographic emulsion measurements of the positive spectrum by Bramson, Havens and Seifert. However Sagane obtains the result $\rho = 0.23 \pm .03$. The latter result has stimulated an exhaustive search for possible systematic errors. For example, the same set of pictures has yielded a mass measurement for the π^- meson which is about 1 percent below the best value.[11] In addition, several long muon tracks were used to obtain the muon mass by residual range in hydrogen vs curvature. Also, $\pi^+ \rightarrow \mu^+$ decays at rest were studied. These serve as an independent and overall calibration of the horizontal scale to better than 3 percent. No other sources of error have been discovered. There is of course the (remote) possibility that the spectra of positive and negative muons are different.[18]

---

[18] W. Panofsky, at the Fifth Annual Rochester Conference, presented

results of K. Crowe at Stanford on positive muons which indicate a value of $\rho = .55 \pm .1$.

Before the present results can be applied to a determination of the beta decay coupling constants, they must be corrected for radiative effects. The inner bremstrahlung contribution has been computed by Lenard.[19] Non radiative corrections of the same order

---

[19] A. Lenard, Phys. Rev. 90, 968 (1953)

---

have recently been examined.[20] We have estimated that these ef-

---

[20] R. Finkelstein and R. Behrends, Phys. Rev. 97, 568 (1955)

---

fects would increase ρ by approximately .04. Thus the value of ρ obtained from this experiment is $0.68 \pm .11$, where the error has been increased to allow for the uncertainty in the radiative corrections. Michel and Wightman[21] have discussed the implications

---

[21] L. Michel and A. Wightman, Phys. Rev. 93, 354 (1954)

---

of the knowledge of ρ on the beta decay coupling constants, assuming the usual connections between Fermi interactions. The muon decay spectrum shape may be used to give some information as to the importance of the pseudoscalar component and as to the relative sign of the scalar and tensor interactions. This information is beset by ambiguities of (1) the distinguishability or indistinguishability of the neutrinos in equation (1) and, (2) the correspondence of the four Fermi particles in nuclear beta decay (pnev) to those in muon decay ($\nu\mu e\nu$, $\mu\nu e\nu$ etc.). The acceptable solutions are listed in Table 2. The input data are: $|g_s/g_t| = 0.85 \pm .13$, $\sigma = \frac{2^8 B}{\mu^5 \tau_\mu \log 2} = 1.22 \pm .05$, $\rho = 0.68 \pm .11$.[22]

0390 012

[22] J. B. Gerhart, Phys. Rev. 95, 288 (1954); O. Kofoed-Hansen and A. Winther, Phys. Rev. 86, 428 (1952) and O. Kofoed-Hansen, private communication.

The authors wish to thank Dr. L. Michel, O. Kofoed-Hansen and J. Steinberger for helpful conversations on this problem.

APPENDIX

A. Angle Measurements

The bottom of the diffusion chamber contains a black glass disc upon which is scribed a grid of fiduciary lines. In measurement the image of the grid is projected onto a rear surface screen at unity magnification. It is generally possible to reproduce all fiduciary dimensions to one part in two hundred.

The camera lens axes are 10 inches apart and intersect the black glass normally. The lenses are 133.5 cm above the glass. The three-dimensional information required for analytical reconstruction of events in space is knowledge of the height z of points on a track above the black glass. Let View A be the reprojection of the picture taken by the camera whose lens axis intersects the black glass at A, with a corresponding definition of View B. Let the displacement in View A of a point on a track from a line DE, perpendicular to AB, be $d_A$cm, and that in View B be d_B. Then the height z in cm above the black glass of the point on the track is related to $d=d_A-d_B$ by: $z=131.0\ d/(25.40+d)$. 131.0 appears in the numerator instead of 133.5 as a result of the effect introduced by the 2.5 inch thick top glass of the chamber. The dip angle of a track is the angle between the tangent to the track and a horizontal plane. z_1 and z_2 are the heights above the black glass of two points 1 and 2 on a track and s is the projected arc length between 1 and 2 as measured in, say, View A. $\Delta z=z_2-z_1$. Then approximately,

$$\tan \alpha=(\Delta a/S)[1+(z_1+z_2)/2\mathrm{x}131.0)+(\Delta z'/s)(b/131.0)]$$

where b cm is the distance, measured in the direction tangent to the track from A to the point on the track halfway between 1 and 2. b is positive if the track is going up as one proceeds along it away from A. If one used View B, s and b would in general be different, but the resulting tan α should be the same. The first correction term is a magnification correction on s, reflecting the fact that when the reprojection magnification is adjusted to be correct for distances on the black glass projected distances between points above the glass appear too large. The second correction term is the conical reprojection correction to first order in tan α/131.0. The above expression for tan α is adequate for this experiment. Δz may ordinarily be measured to 0.15 cm.

B. MOMENTUM MEASUREMENTS

A singly charged particle with momentum p and dip angle α moving in a uniform vertical magnetic field of H kilogauss traverses a right circular helix characterized by pitch angle α and ρ radius. P in Mev/c is related to ρ and α by $p = 0.3\ H\rho/\cos\alpha$, where ρ is measured in cm. Ordinarily in this work 5 cm $<\rho<$ 60 cm and ρ', apparent ρ, is satisfactorily measured by fitting a ruled circular template to the reprojected track. ρ and ρ' are related by

$$\rho = \rho'[1- \frac{z}{131.0} - \frac{2b\tan\alpha}{131.0} + (3b^2 + 1/2\ a^2)\ \tan^2\alpha/(131)^2]$$

The symbols have the same meaning and the corrections the same origin as in the expression for tan α. ρ' has reference to the radius of curvature of the reprojected track at a single point and z is the height of that point above the black glass. 'a' is the distance to the appropriate fiduciary mark measured perpendicular to the track. In the measurement of the μ decay spectrum the median correction of ρ corresponding to the last term was 0.2 percent. The equation is correct through terms of the second order of cloud chamber dimensions modulated by tan α and divided by 131 cm. The use of a finite length of track to measure ρ implies an additional correction of first order in $|\tan \alpha|$, a correction which becomes increasingly important as ρ becomes smaller. For ρ sufficiently small it makes the template method of measurement inappropriate.

The multiple scattering uncertainty may be calculated. The possible magnitude of photographic and reprojection distortion effects has been checked by photographing ruled templates and has been found to be determined essentially only by the fidelity with which one can reproduce in reprojection the correct relative position of the fiduciary marks. With moderate care the uncertainty in momentum due to this effect is a small fraction of a percent.

On occasion the magnetic field was reduced to 120 gauss and the absorber external to the chamber was removed. Most of the particles then photographed would be mesons with a most probable energy of about 65 Mev, or momentum of about 150 Mev/c. Some mesons with decidedly lower momentum and occasional protons and electrons would also be present. The small residual field serves to identify low momentum tracks whose multiple scattering would otherwise be interpreted as distortion.

The results of this series of photographs lead to the conclusion that for long, flat tracks the turbulence induced radii of curvature are probably greater than 100 meters.

C. MOMENTUM-RESOLUTION OF THE μ DECAY SPECTRUM

The visible length of most of the decay electron tracks is less than 15 cm. For such short tracks the measurement error in the radius of curvature ρ is larger than 1 percent and it makes the major contribution to the total uncertainty of the momentum measurement. In order to assign a standard error to each momentum measurement an estimate of the measurement error was made for each event.

The resolution function $R_2(p,p')$ represents the probability per unit momentum interval of observing electrons with momentum p' if the actual momentum of all electrons is p. If $Q(\sigma)$ represents the probability distribution function of standard momentum errors for all events with momenta roughly equal to p, then an estimate of $R(p,p')$ is:

$$R_2(p,p') = 1/2\pi \int_0^\infty Q(\sigma) e^{-(p-p')^2/2\sigma^2} d\sigma$$

$R_2(p,p')$ was found for p = 20, and 50 Mev/c using events with momenta between 15 and 25, 45 and 55 Mev/c respectively to find $Q(\sigma)$. The resolution functions for p = 20 and 50 Mev/c are shown on Fig. 2 for all events and on Fig. 3 for the more restricted data.

For the 2 values of p the shapes of R(p,p') are very closely identical and the half-widths are nearly proportional to p, The uncertainty in the value of the resolution width is quite large (perhaps of the order of 35 percent) because of the arbitrary nature of the assignment of standard measurement errors to the individual events.

FIGURE CAPTIONS

FIGURE

1. Diffusion Cloud Chamber photograph of the decay of a negative muon.

2. Spectrum of electrons from muon decay. A total of 415 events were used. The 'poor' resolution curves are given above the spectrum at 20 and 50 Mev.

3. Spectrum of electrons using 'good' resolution. This spectrum includes 282 events which survive the more restrictive criteria designed to yield longer, flatter tracks.

4. Theoretical spectra for muon decay. The Michel curves for $\rho = 0$, .25, .50, .75 and 1.00 are folded with the experimental resolution of Fig. 2. The poor resolution experimental points are also shown.

5. Chi-square minimum method of estimated ρ from the data of Fig. 2. The probability that chi-square exceeds the value given by the ordinate is also indicated (from Cramer, Mathematical Methods of Statistics, Princeton, 1951). Momentum intervals with statistics of fewer than 10 events were pooled to obtain a total of 18 intervals. The number of degrees of freedom for the normalized distribution with one parameter is 16.

TABLE 1

Determination of ρ by Moments

	ρ	$\Delta\rho_H$	$\Delta\rho_s$
1st Moment			
Good Resolution[a]	.67	+.05	.11
Poor Resolution[b]	.60		.09
2nd Moment			
Good Resolution	.68	+.06	.11
Poor Resolution	.64		.09
Split First Moment			
$0 \leq x \leq .75$	.72	−.03	.19
$.75 \leq x \leq \infty$	.69	+.02	.18

a) 282 events; see Fig. 3

b) 415 events; see Fig. 2

TABLE II[a]

Beta Interaction Coupling Constants[a]

	Identical Neutrinos		Distinguishable Neutrinos	
Correspondence:	$pne\nu \to \nu\mu e\nu$	$pne\nu \to \mu\nu e\nu$	$pne\nu \to \nu\mu e\nu$	$pne\nu \to \mu\nu e\nu$
g_p/g_t	+.5 ±.5	+.5 ± .5	+4.5±.5	+4.5+.5
g_s/g_t	negative	positive	positive	negative

a) See Ref. 19 for notation.

21

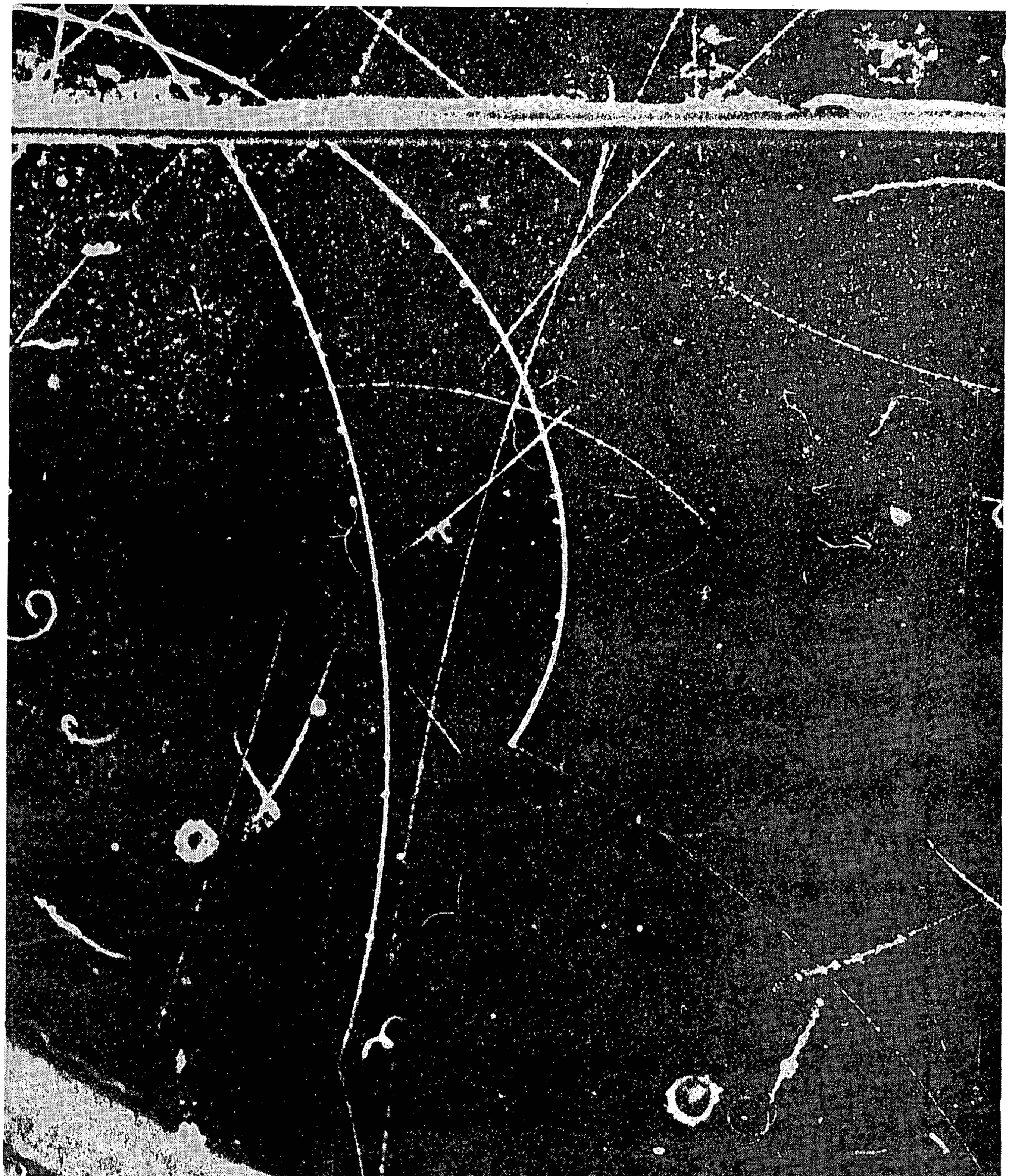

0390 022

22

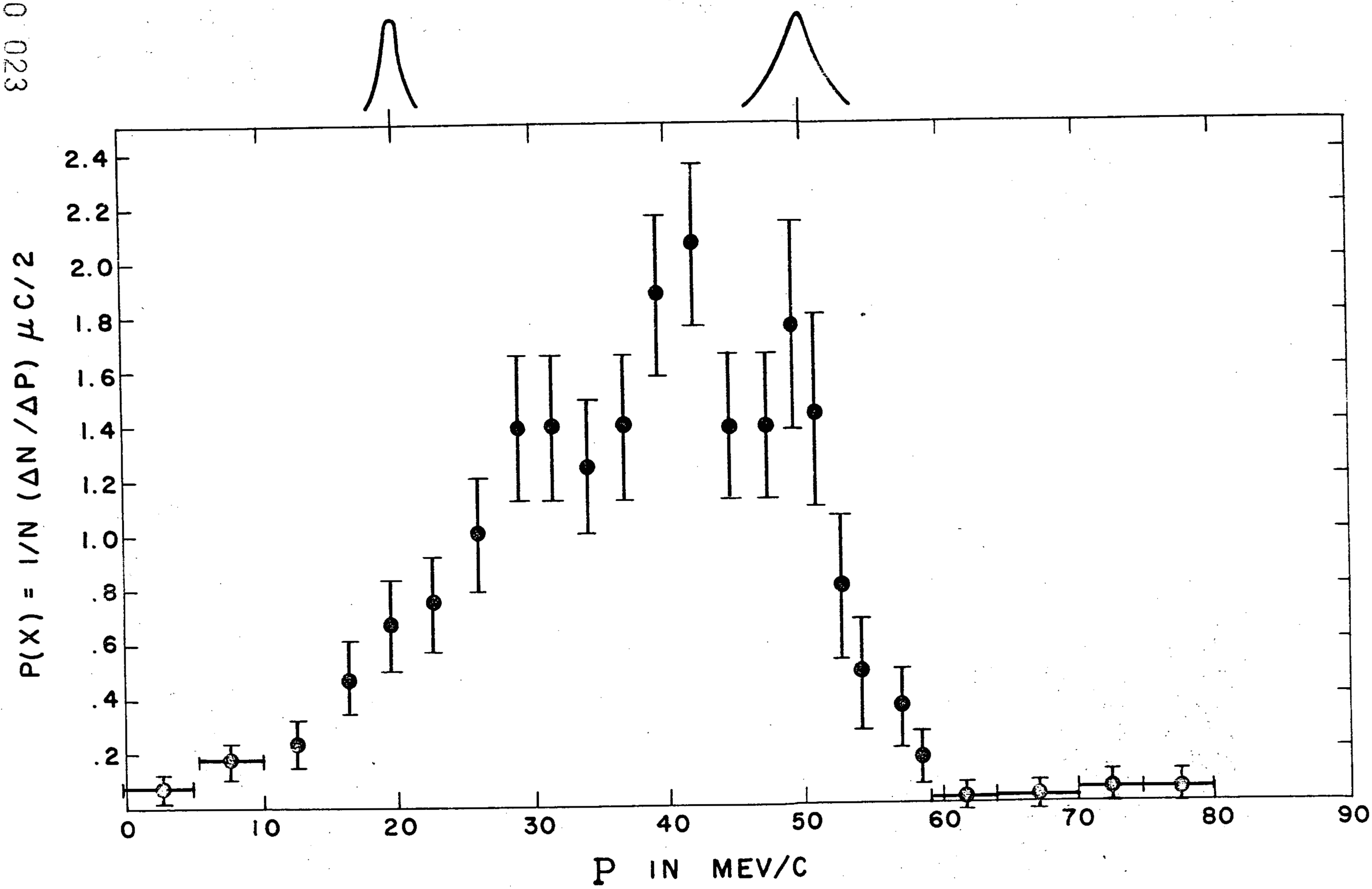
P(X) = 1/N (ΔN / ΔP) μC/2
2.4
2.2
2.0
1.8
1.6
1.4
1.2
1.0
.8
.6
.4
.2
0
10
20
30
40
50
60
70
80
90
P IN MEV/C

0390 023

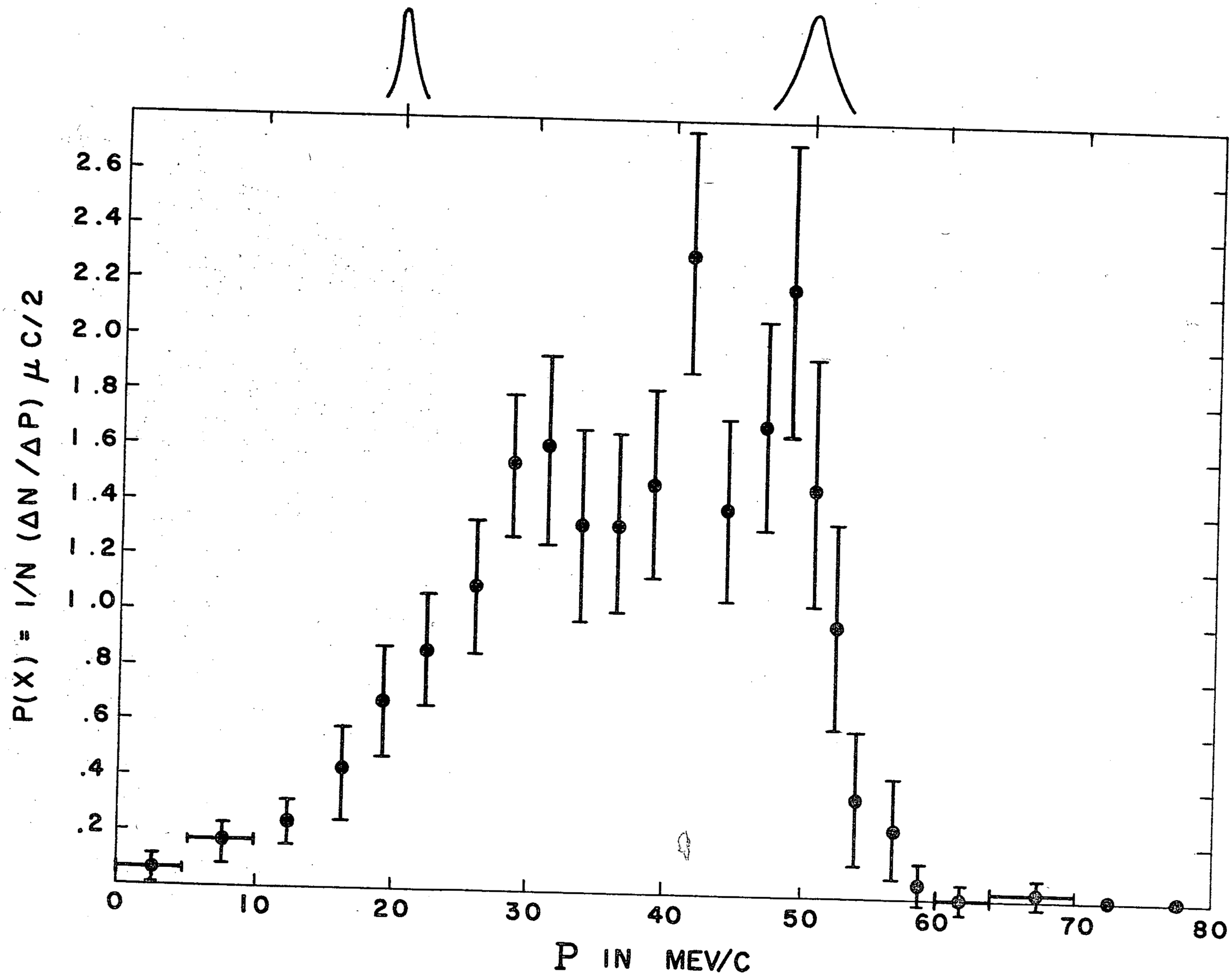

P(X) = 1/N (ΔN/ΔP) μC/2
2.6
2.4
2.2
2.0
1.8
1.6
1.4
1.2
1.0
.8
.6
.4
.2
0
10
20
30
40
50
60
70
80
P IN MEV/C

0390 024

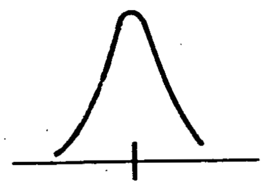

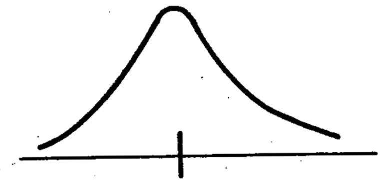

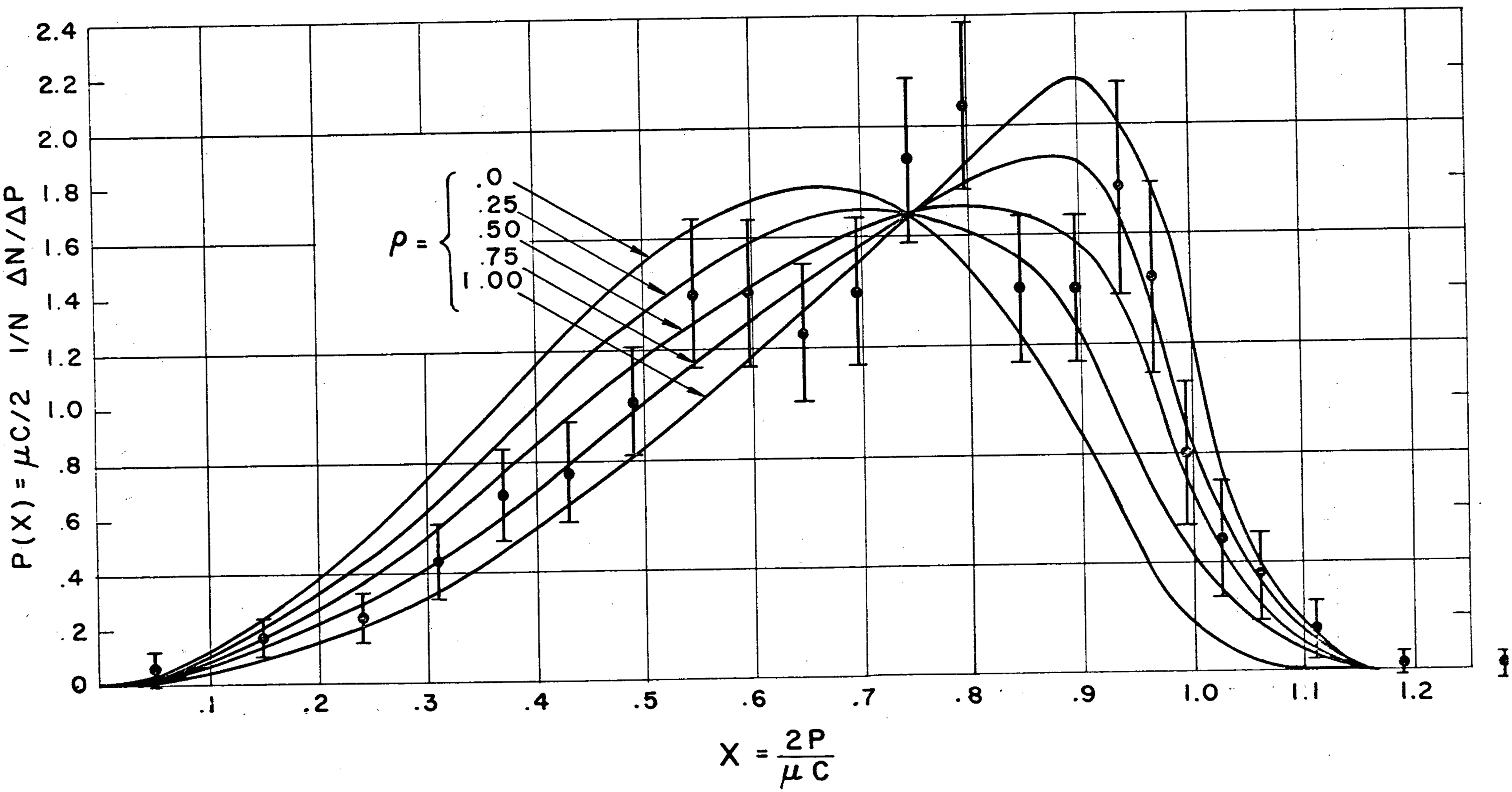

P(X) = μC/2 1/N ΔN/ΔP
2.4
2.2
2.0
1.8
1.6
1.4
1.2
1.0
.8
.6
.4
.2
0
.1
.2
.3
.4
.5
.6
.7
.8
.9
1.0
1.1
1.2
ρ =
.0
.25
.50
.75
1.00
X = 2P/μC

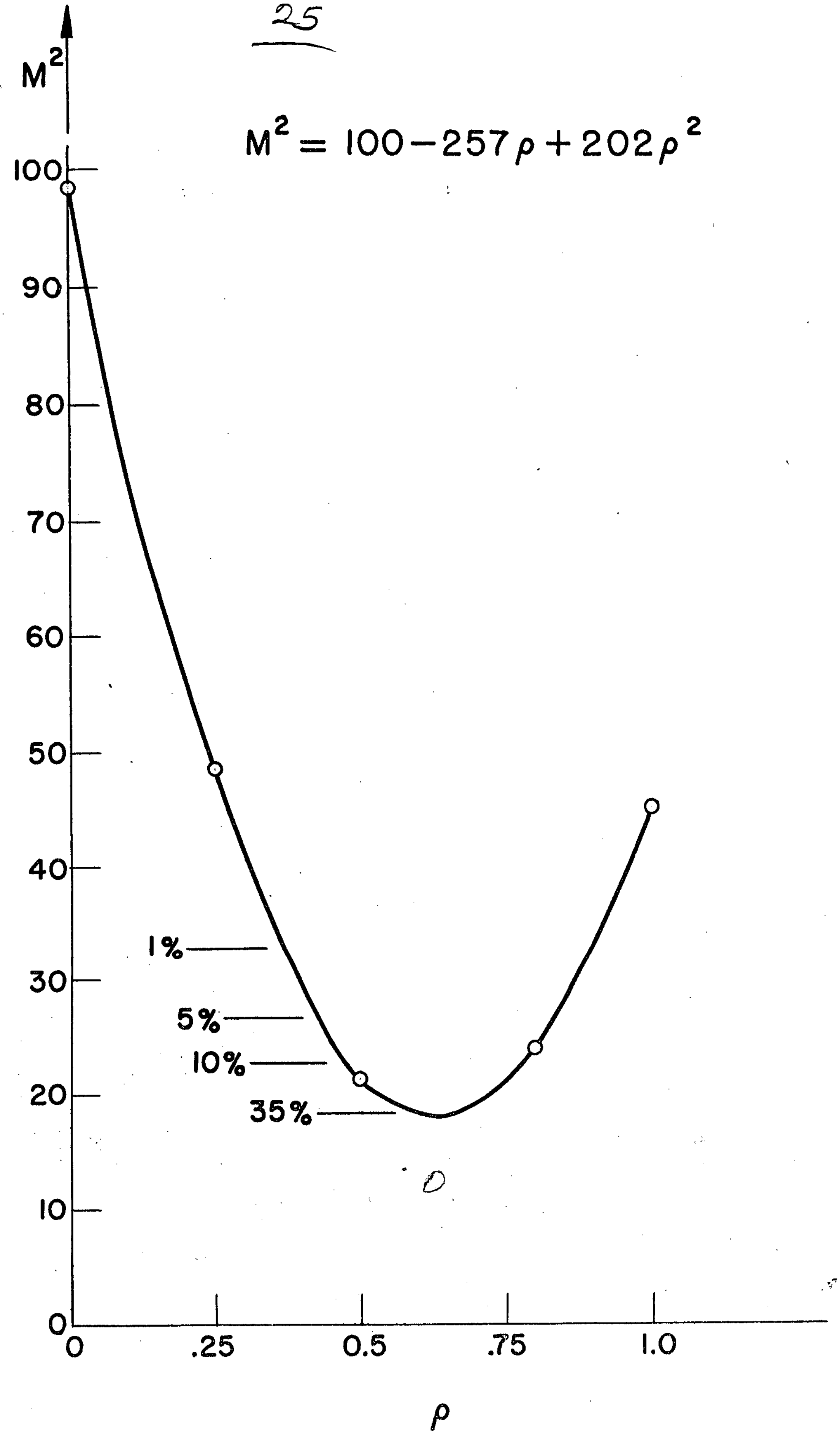

M^2
$M^2 = 100 - 257\rho + 202\rho^2$
100
90
80
70
60
50
40
30
20
10
0
1%
5%
10%
35%
0
.25
0.5
.75
1.0
ρ

0390 026